Medicinal Chemistry Research
https://doi.org/10.1007/s00044-018-2255-0

MEDICINAL CHEMISTRY RESEARCH

ORIGINAL RESEARCH

Synthesis and spectroscopic analysis of benzylidene imidazolone linked to P-porphyrins through axial ligand

Jin Matsumoto[1] · Kyosuke Takemori[1] · Jun Ishikawa[1] · Yu Nabetani[1] · Mamoru Fujitsuka[2] · Tetsuro Majima[2] · Masahide Yasuda[1]

Received: 24 May 2018 / Accepted: 19 October 2018

Abstract

Tetraphenylporphyrinatophosphorus(V) complexes (**1**) comprising two axially linked benzylidene imidazolone (Biz) moieties, which are chromophores of the green fluorescent protein, were prepared. In medical applications such as photodynamic therapy, the P-porphyrin part (Ptp) is expected to sensitize to generate singlet oxygen, whereas the Biz units act as fluorescent probes. The fluorescence spectra of **1** were analyzed under the excitations of Biz at 370 nm. Fluorescence stemming from the excited states of Biz and Ptp was observed at 460 and 610 nm, respectively. The intramolecular quenching of Biz in the excited singlet state by Ptp occurred, resulting in weak fluorescence from Biz. The introduction of a cyano group in the Biz units of **1** enhanced their fluorescence quantum yield up to 7.7×10^{-4}. The fluorescence spectra of **1** under the excitations of Ptp at 550 nm were extremely similar to that of a reference compound of P-porphyrin without the Biz chromophore, dimethoxy(tetraphenylporphyrinato)phosphorus chloride. The physicochemical parameters of Ptp remained unaltered following the introduction of Biz on the axial positions of P-porphyrin.

Keywords Benzylidene imidazolone · P-porphyrin · Intermolecular electron transfer · Fluorescent probe

Introduction

Photodynamic therapy (PDT) has become a well-recognized cancer therapy that uses singlet-oxygen photosensitizers such as porphyrin derivatives (Dąbrowski et al. 2016; Gomer and Ferrario 1990; Mehraban and Freeman 2015). In PDT, the porphyrin derivatives function as both sensitizers and fluorescent probes (Ethirajan et al. 2011; Josefsen and Boyle 2012). These sensitizers are required to absorb in the optical window between 650 and 850 nm to avoid interference with absorption of light by tissue chromophores (Plaetzer et al. 2009). This causes difficulties in detecting the presence of these sensitizers in tumor by fluorescence, which shifts from visible region to near infrared region. With the aim of overcoming this problem, we intended to develop a porphyrin bearing a second chromophore that acted as a fluorescent probe. Previously, we have extensively studied the photodynamic activity of phosphorus porphyrins (P-porphyrins) using *Saccharomyces cerevisiae* (Matsumoto et al. 2016; Matsumoto et al. 2011), *E. coli* (Matsumoto et al. 2017a; Matsumoto et al. 2017b), and cancer cells (Matsumoto et al. 2017c). On the other hand, the green fluorescent protein (GFP) is a biologically applicable fluorescent protein that contains a benzylidene imidazolone (Biz) chromophore, which is constructed by the condensation of glycine, tyrosine, and serine (Craggs 2009; Phillips Jr 1997) and whose fluorescence properties can be tuned via chemical modifications (Follenius-Wund et al. 2003; Walker et al. 2015). Bearing this in mind, we selected the Biz chromophore as the second fluorescent probe, which was connected to a P-porphyrin complex through linkers (L) in the axial positions, affording P-

✉ Jin Matsumoto
jmatsu@cc.miyazaki-u.ac.jp

[1] Department of Applied Chemistry, Faculty of Engineering, University of Miyazaki, Gakuen-Kibanadai, Miyazaki 889-2192, Japan

[2] The Institute of Scientific and Industrial Research (SANKEN), Osaka University, 8-1 Mihogaoka, Ibaraki, Osaka 567-0047, Japan

Published online: 27 October 2018

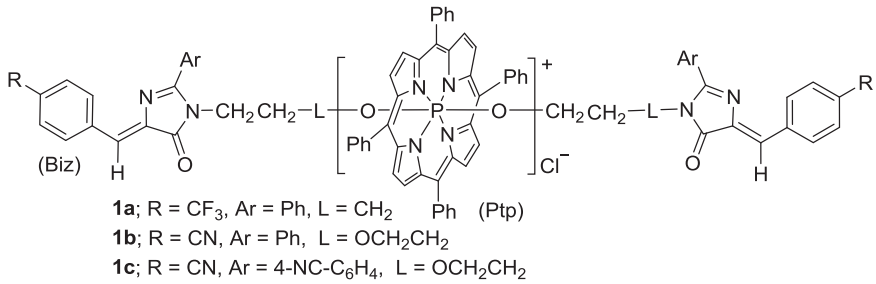

Scheme 1 P-porphyrins **1a**–**1c** having benzylidene imidazolone (Biz) units linked via axial ligands

porphyrins **1a**–**1c** (Scheme 1). Herein, we examined the effects of the substituents (R and Ar) of Biz and L on the fluorescence properties of **1**.

Instruments

^{1}H NMR (400 MHz) and ^{13}C NMR (100 MHz) spectra were recorded with a Bruker AV 400 M spectrometer, using $CDCl_3$ or CD_3OD as solvents and $SiMe_4$ as the internal standard. In ^{13}C NMR, substitution level of each carbon was determined by DEPT method and described as CH_3 (primary), CH_2 (secondary), CH (tertiary and vinyl), and C (quaternary and ipso) in spectral data. High-resolution mass spectra (HRMS) were measured on a Thermo Scientific Q Exactive mass spectrometer equipped with an electrospray ionization source. Absorption spectra were measured in MeOH using a JASCO V-550 spectrophotometer. Redox potentials were determined via cyclic voltammetry in MeCN (10 mM) in the presence of a supporting electrolyte (Et_4NBF_4; 0.1 M); these measurements were performed on a BAS CV-50W cyclic voltammeter at a scan rate of 300 mV s^{-1} at 25 °C using a Pt working electrode, a Pt counter electrode, and an Ag/$AgNO_3$ reference electrode.

Preparation of 4-substituted benzylidene-2-phenyloxazolone (3)

To a solution of *p*-trifluoromethylbenzaldehyde (1.0 mL) in tetrahydrofuran (20 mL), *N*-benzoylglycine(1.0 g), and catalytic $Zn(OAc)_2$ (1.1 g) were added. The reaction mixture was refluxed for 4 h at 80 °C (Scheme 2). After the solvent of the reaction mixture was evaporated under vacuum, water (120 mL) was added and the solution was allowed to stand overnight at room temperature. Compound **3a** was collected from the solution as a precipitate. Following recrystallization from CH_2Cl_2 (100 mL), **3a** was isolated in 80% yield (1.41 g). A similar procedure was followed for the preparation of the other oxazolone derivatives (**3b**–**3d**). The spectral data corresponding to compounds **3a**–**3d** are listed below.

p-Trifluoromethylbenziyidene-5-phenyl-1-oxazolone (3a)

Pale yellowish needles; Yield 80%; mp 171–172 °C ($CHCl_3$–Hexane); IR (KBr) ν_{max} 3044, 1802, 1657, 1558, 1324, 1168 cm^{-1}; ^{1}H NMR $\delta = 7.25$ (s, 1H, -C<u>H</u>=C<), 7.55–7.58 (m, 2H, H-3, and H-5 of C_6H_5), 7.64–7.68 (m, 1H, H-4 of C_6H_5), 7.73 (d, $J = 8.2$ Hz, 2H, H-3, and H-5 of $C_6H_4CF_3$), 8.20–8.22 (m, 2H, H-2, and H-6 of C_6H_5), 8.32 (d, 2H, H-2, and H-6 of $C_6H_4CF_3$); HRMS Calcd for $C_{17}H_{11}F_3NO_2^+$ $[M+H]^+$: 318.0736, *m/z* 318.0736. Found: 318.0726.

p-Cyanobenziyidene-5-phenyl-1-oxazolone (3b)

White powder; Yield 40%; mp > 157 °C (dec); IR (KBr) ν_{max} 3066, 2222, 1796, 1661, 1561, 1165 cm^{-1}; ^{1}H NMR $\delta = 7.20$ (s, 1H, -C<u>H</u>=C<), 7.55–7.59 (m, 2H, H-3, and H-5 of C_6H_5), 7.65–7.70 (m, 1H, H-4 of C_6H_5), 7.76 (d, $J = 8.4$ Hz, 2H, H-3, and H-5 of C_6H_4CN), 8.19–8.23 (m, 2H, H-2, and H-6 of C_6H_5), 8.31 (d, $J = 8.4$ Hz, 2H, H-2, and H-6 of C_6H_4CN); HRMS Calcd for $C_{17}H_{11}N_2O_2^+$ $[M+H]^+$: 275.0815, *m/z* 275.0815. Found: 275.0809.

p-Cyanobenziyidene-5-(4-cyanophenyl)-1-oxazolone (3c)

Pale yellow solid; Yield 52%. ^{1}H NMR $\delta = 7.30$ (s, 1H, -C<u>H</u>=C<), 7.77–7.89 (m, 2H, H-3, and H-5 of C_6H_4CN on olefin), 7.85–7.88 (m, 2H, H-3, and H-5 of C_6H_4CN on oxazolone), 8.29–8.31 (m, 2H, H-2, and H-6 of C_6H_4CN on olefin), 8.31 (d, $J = 8.4$ Hz, 2H, H-2, and H-6 of C_6H_4CN on oxazolone).

p-Hydroxybenziyidene-5-phenyl-1-oxazolone (3d)

Yellow powder; Yield 50%; mp > 180 °C (dec); IR (KBr) ν_{max} 3443, 3069, 1752, 1656, 1557, 1362, 1165 cm^{-1}; ^{1}H NMR $\delta = 6.93$–6.95 (m, 2H, H-3, and H-5 of C_6H_4-OH), 7.22 (s, 1H, -C<u>H</u>=C<), 7.51–7.55 (m, 2H, H-3, and H-5 of C_6H_5), 7.58–7.63 (m, 1H, H-4 of C_6H_5), 8.15–8.18 (m, 2H, H-2, and H-6 of C_6H_4OH), 8.16–8.19 (m, 2H, H-2, and H-6 of C_6H_5); HRMS Calcd for $C_{16}H_{12}NO_3^+$ $[M+H]^+$: 266.0812, *m/z* 266.0812. Found: 266.0807.

Scheme 2 Synthetic routes of **2a–2d** and **1a–1c**

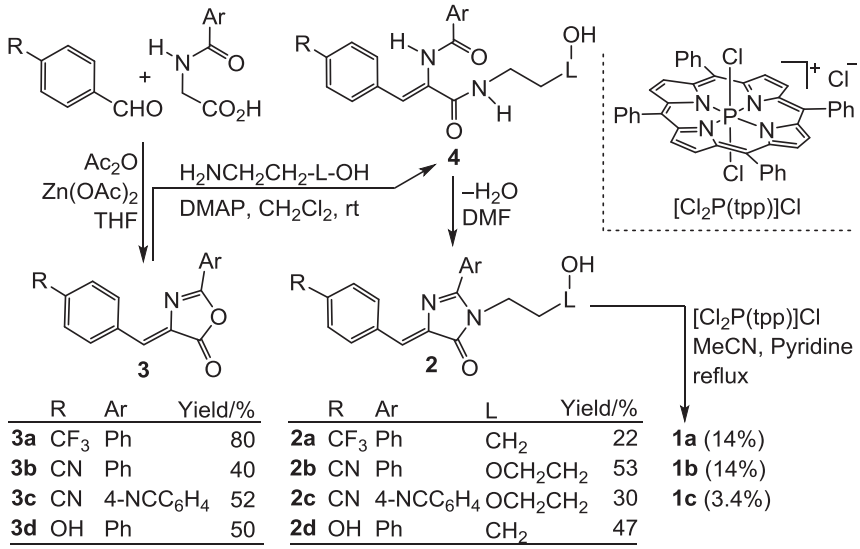

	R	Ar	Yield/%
3a	CF_3	Ph	80
3b	CN	Ph	40
3c	CN	4-NCC_6H_4	52
3d	OH	Ph	50

	R	Ar	L	Yield/%
2a	CF_3	Ph	CH_2	22
2b	CN	Ph	OCH_2CH_2	53
2c	CN	4-NCC_6H_4	OCH_2CH_2	30
2d	OH	Ph	CH_2	47

General procedure for the preparation of imidazolone derivatives 2

The linker was introduced via aminolysis of **3a** with 3-amino-1-propanol (70 μL) in the presence of 4-(dimethylamino)pyridine (DMAP, 10.8 mg) in CH_2Cl_2 (6.0 mL) at room temperature for 24 h to afford **4a** (R=CF_3, Ar=Ph, L=OCH_2CH_2) in 98% yield (340 mg). Crude **4a** (200 mg) was heated in DMF (10 mL) at 180 °C for 6 h in a pressure bottle, affording a crude residue, which was purified via column chromatography on silica gel to yield **2a** (120 mg, 51%). Other imidazolone derivatives **2b–2d** were prepared following a similar procedure. For **2b** and **2c**, 2-(2-aminoethoxy)ethanol (70 μL) was used for aminolysis instead of 3-amino-1-propanol. The spectral data of **2a–2d** are listed below.

3-[3-(*p*-Trifluoromethylbenzylidene)-5-phenyl-1-imidazolonyl]propanol (2a)

Orange solid. Yield 17%; mp = 99–101 °C; IR (KBr) ν_{max} 3400, 2931, 1715, 1645, 1325, 1165, 1070 cm^{-1}; ^1H NMR δ = 1.80–1.86 (m, 2H, -$CH_2CH_2CH_2OH$), 3.62 (t, J = 5.7 Hz, 2H, -$CH_2CH_2C\underline{H}_2OH$), 3.95 (t, J = 6.5 Hz, 2H, -$C\underline{H}_2CH_2CH_2OH$), 7.26 (s, 1H, -C$\underline{H}$=C<), 7.54–7.64 (m, 3H, H-3, H-4, and H-5 of C_6H_5 on Biz), 7.67 (d, J = 8.4 Hz, 2H, H-3, and H-5 of $C_6H_4CF_3$), 7.82–7.84 (m, 2H, H-2, and H-6 of C_6H_5 on Biz), 8.33 (d, J = 8.4 Hz, 2H, H-2, and H-6 of $C_6H_4CF_3$); HRMS Calcd for $C_{20}H_{18}F_3N_2O_2^+$ $[M+H]^+$: 375.1315, *m/z* 375.1315. Found: 375.1315.

5-[3-(*p*-Cyanobenzylidene)-5-phenyl-1-imidazolonyl]-3-oxypentanol (2b)

Yellow powder. Yield 20%; mp = 120–121 °C; IR (KBr) ν_{max} 3425, 2939, 2226, 1715, 1646, 1165, 1051 cm^{-1}; ^1H NMR δ = 3.45–3.48 (m, 2H, -$OC\underline{H}_2CH_2OH$), 3.59–3.62 (m, 2H, -$OCH_2C\underline{H}_2OH$), 3.66 (t, J = 5.4 Hz, 2H, >$NCH_2C\underline{H}_2O$-), 4.04 (t, J = 5.4 Hz, 2H, >$NC\underline{H}_2CH_2O$-), 7.18 (s, 1H, -C$\underline{H}$=C<), 7.54–7.64 (m, 3H, H-3, H-4, and H-5 of C_6H_5 on Biz), 7.68–7.70 (m, 2H, H-3, and H-5 of C_6H_4CN), 7.87–7.90 (m, 2H, H-2, and H-6 of C_6H_5 on Biz), 8.31–8.32 (m, 2H, H-2, and H-6 of C_6H_4CN); HRMS Calcd for $C_{21}H_{20}N_3O_3^+$ $[M+H]^+$: 362.1499, *m/z* 362.1499. Found: 362.1496.

5-[3-(*p*-Cyanobenzylidene)-5-(4-cyanophenyl)-1-imidazolonyl)-3-oxypentanol (2c)

Yellow powder. Yield 12% (10% from *p*-cyanobenzaldehyde), mp > 176 °C (dec); IR (KBr) ν_{max} 3425, 2959, 2227, 1720, 1644, 1165, 1053 cm^{-1}; ^1H NMR δ = 3.49 (t, J = 4.9 Hz, 2H, -$OC\underline{H}_2CH_2OH$), 3.63 (t, J = 4.9 Hz, 2H, -$OCH_2C\underline{H}_2OH$), 3.78 (t, J = 5.1 Hz, 2H, >$NCH_2C\underline{H}_2O$-), 3.93 (t, J = 5.1 Hz, 2H, >$NC\underline{H}_2CH_2O$-), 7.22 (s, 1H, -C$\underline{H}$=C<), 7.69–7.71 (m, 2H, H-3, and H-5 of C_6H_4CN on olefin), 7.82–7.84 (m, 2H, H-3, and H-5 of C_6H_4CN on Biz), 8.18–8.20 (m, 2H, H-2, and H-6 of C_6H_4CN on Biz), 8.29–8.30 (m, 2H, H-2, and H-6 of C_6H_4CN on olefin); HRMS Calcd for $C_{22}H_{19}N_4O_3^+$ $[M+H]^+$: 387.1452, *m/z* 387.1452. Found: 387.1453.

3-[3-(*p*-Hydroxybenzylidene)-5-phenyl-1-imidazolonyl] propanol (2d)

Yellow powder. Yield 22%; mp > 153 °C (dec); IR (KBr) ν_{max} 3349, 3150, 2946, 1682, 1640, 1377, 1293, 1172, 1161, 1057 cm^{-1}; ^1H NMR δ = 1.74–1.82 (m, 2H, -$CH_2C\underline{H}_2CH_2OH$), 3.51 (t, J = 6.0 Hz, 2H, -$C\underline{H}_2CH_2CH_2OH$), 3.90 (t, J = 7.6 Hz, 2H, -$CH_2CH_2C\underline{H}_2OH$), 6.85 (d, J = 8.8 Hz, 2H, H-3, and H-5 of C_6H_4OH), 7.19 (s, 1H, -C$\underline{H}$=C <), 7.56-7.63 (m, 3H, H-3,

H-4, and H-5 of C_6H_5), 7.83–7.85 (m, 2H, H-2, and H-6 of C_6H_5 on Biz), 8.12 (d, $J = 8.8$ Hz, 2H, H-2, and H-6 of C_6H_4OH); HRMS Calcd for $C_{19}H_{17}N_2O_3^-$ $[M-H]^-$: 321.1245, *m/z* 321.1245. Found: 321.1245.

Preparation of P-porphyrins (1a–1c) with benzylidene imidazolone (Biz) units linked through the axial ligands

1a was prepared by heating tetraphenylporphyrinato (dichloro)phosphorus(V) chloride ($[Cl_2P(tpp)]Cl$, 30 mg) with **2a** (200 mg) in a mixed solvent of MeCN (10 mL) and pyridine (1.0 mL) at 110 °C for 5 days in a pressure bottle. The crude product was purified via column chromatography on silica gel to afford **1a** (8.0 mg) in 14% yield. Similarly, **1b** and **1c** were prepared from **2b** and **2c**, respectively.

Bis[3-{3-(*p*-trifluoromethylbenzylidene)-5-phenyl-1-imidazolonyl}propyloxo] tetraphenylporphyrinatophosophorus chloride (1a)

Purple solid. Yield 14%. mp > 300 °C; IR (KBr) ν_{max} 3058, 2931, 1714, 1644, 1323, 1168, 1124, 1068, 1022, 803, 758, 702 cm^{-1}; ^1H NMR $\delta = -2.47$ (dt, $J_{P-H} = 14.5$ Hz, $J = 6.5$ Hz, 4H, P-OC$\underline{H}_2$-), -1.27 (t, $J = 6.5$ Hz, 4H, P-OCH$_2$C$\underline{H}_2$-), 1.84 (t, $J = 6.5$ Hz, 4H, P-OCH$_2$CH$_2$C$\underline{H}_2$-), 6.66 (s, 2H, -C$\underline{H}$=C<), 6.83–6.85 (m, 4H, H-2, and H-6 of C_6H_5 on Biz), 7.07–7.10 (m, 4H, H-3, and H-5 of C_6H_5 on Biz), 7.35–7.39 (m, 2H, H-2 of C_6H_5 on Biz), 7.65–7.71 (m, 8H, H-3, and H-5 of C_6H_5 at *meso* position), 7.71 (d, $J = 8.3$ Hz, 2H, H-3, and H-5 of $C_6H_4CF_3$), 7.74–7.78 (m, 4H, H-4 of C_6H_5 at *meso* position), 7.82–7.84 (m, 8H, H-2, and H-6 of C_6H_5 at *meso* position), 8.19 (d, $J = 8.3$ Hz, 2H, H-2 and H-6 of $C_6H_4CF_3$), 8.99 (d, $J_{P-H} = 2.8$ Hz, 8H, pyrrole β); ^{13}C NMR: $\delta = 26.66$ (CH_2, d, $J_{P-C} = 15.2$ Hz, P-O-CH$_2$-C$\underline{H}_2$-), 37.16 (CH_2, P-O-CH$_2$-CH$_2$-C$\underline{H}_2$-), 59.03 (CH_2, d, $J_{P-C} = 14.1$ Hz, P-O-C$\underline{H}_2$-), 116.19 (C, *meso* of porphyrin ring), 123.89 (C, q, $J_{F-C} = 271.8$ Hz, -CF_3), 125.48 (CH, -C$\underline{H}$=C<), 125.67 (CH, q, $J_{F-C} = 3.7$ Hz, C-3, and C-5 of $C_6H_4CF_3$), 127.57 (CH, C-2, and C-6 of C_6H_5 on Biz), 127.71 (C, C-1 of C_6H_5 on Biz), 128.45 (CH, C-3, and C-5 of C_6H_5 at *meso* position), 128.59 (CH, C-3 and C-5 of C_6H_5 on Biz), 129.76 (CH, C-4 of C_6H_5 at *meso* position), 131.46 (C, q, $J_{F-C} = 32.5$ Hz, C-4 of $C_6H_4CF_3$), 131.76 (CH, C-4 of C_6H_5 on Biz), 132.37 (CH, C-2, and C-6 of $C_6H_4CF_3$), 133.11 (CH, d, $J_{P-C} = 5.1$ Hz, pyrrole β), 133.50 (CH, C-2, and C-6 of C_6H_5 at *meso* position), 135.09 (C, C-1 of C_6H_5 at *meso* position), 137.32 (C, C-1 of $C_6H_4CF_3$), 139.15 (C, C-3 of imidazolone), 139.23 (C, pyrrole α), 162.08 (C, C-5 of imidazolone), 169.72 (C, C-2 of imidazolone); ^{19}F NMR (376 MHz): $\delta = -62.82$; HRMS Calcd for $C_{84}H_{60}F_6N_8O_4P^+$ $[M^+]$: 1389.4374, *m/z* 1389.4374. Found: 1389.4401.

Bis[5-{3-(*p*-cyanobenzylidene)-5-phenyl-1-imidazolonyl}-3-oxypentyloxo]tetraphenylporphyrinatophosophorus chloride (1b)

Purple solid. Yield 14%. mp > 300 °C; IR (KBr) ν_{max} 3057, 2939, 2226, 1714, 1644, 1022, 803, 759, 704 cm^{-1}; ^1H NMR $\delta = -2.30$ (dt, $J_{P-H} = 12.4$ Hz, $J = 5.2$ Hz, 4H, P-OC$\underline{H}_2$-), 0.56–0.59 (m, 4H, P-OCH$_2$C$\underline{H}_2$-), 2.33 (t, $J = 5.4$ Hz, 4H, -O C$\underline{H}_2$CH$_2$N-), 2.91 (t, $J = 5.4$ Hz, 4H, -OCH$_2$C$\underline{H}_2$N-), 6.80 (s, 2H, -C$\underline{H}$=C<), 6.84–6.88 (m, 4H, H-3, and H-5 of C_6H_5 on Biz), 6.92–6.94 (m, 4H, H-2, and H-6 of C_6H_5 on Biz), 7.37–7.41 (m, 2H, H-2 of C_6H_5 on Biz), 7.69–7.78 (m, 8H, H-3, H-4, and H-5 of C_6H_5 at *meso* position), 7.71 (d, $J = 8.3$ Hz, 2H, H-3, and H-5 of C_6H_4CN), 7.85–7.87 (m, 8H, H-2, and H-6 of C_6H_5 at *meso* position), 8.24 (d, $J = 8.3$ Hz, 2H, H-2, and H-6 of C_6H_4CN), 8.94 (d, $J_{P-H} = 2.9$ Hz, 8H, pyrrole β); ^{13}C NMR: $\delta = 40.95$ (CH_2, -O-CH$_2$-C$\underline{H}_2$-N), 60.31 (CH_2, d, $J_{P-C} = 15.2$ Hz, P-O-C$\underline{H}_2$-CH$_2$-), 66.60 (CH_2, O-C$\underline{H}_2$-CH$_2$-N), 66.85 (CH_2, d, $J_{P-C} = 18.3$ Hz, P-O-CH$_2$C$\underline{H}_2$-), 112.88 (C, C-4 of C_6H_4CN), 116.28 (C, *meso* of porphyrin ring), 118.63 (C, -$\underline{C}$N), 124.92 (CH, -$\underline{CH}$=C<), 128.10 (C, C-1 of C_6H_5 on Biz), 128.32 (CH, C-2, and C-6 of C_6H_5 on Biz), 128.32 (CH, C-3, and C-5 of C_6H_5 on Biz), 128.57 (CH, C-3, and C-5 of C_6H_5 at *meso* position), 129.84 (CH, C-4 of C_6H_5 at *meso* position), 131.50 (CH, C-4 of C_6H_5 on Biz), 132.30 (CH, C-3, and C-5 of C_6H_4CN), 132.38 (CH, C-2, and C-6 of C_6H_4CN), 133.05 (CH, d, $J_{P-C} = 5.3$ Hz, pyrrole β), 133.46 (CH, C-2, and C-6 of C_6H_5 at *meso* position), 135.14 (C, C-1 of C_6H_5 at *meso* position), 138.41 (C, C-1 of C_6H_4CN), 139.08 (C, pyrrole α), 140.46 (C, C-3 of imidazolone), 164.13 (C, C-5 of imidazolone), 170.78 (C, C-2 of imidazolone); HRMS Calcd for $C_{86}H_{64}N_{10}O_6P^+$ $[M^+]$: 1363.4742, *m/z* 1363.4742. Found: 1363.4763.

Bis[5-{3-(*p*-cyanobenzylidene)-5-(*p*-cyanophenyl)-1-imidazolonyl}-3-oxypentyloxo] tetraphenylporphyrinatophosophorus chloride (1c)

Purple solid. Yield 3.4%. mp > 300 °C; IR (KBr) ν_{max} 3058, 2959, 2226, 1716, 1661, 1443, 1384, 1022, 804, 759, 703 cm^{-1}; ^1H NMR $\delta = -2.23$ (dt, $J_{P-H} = 13.3$ Hz, $J = 4.8$ Hz, 4H, P-OC$\underline{H}_2$-), 0.63–0.66 (m, 4H, P-OCH$_2$C$\underline{H}_2$-), 2.43 (t, $J = 4.9$ Hz, 4H, -OC$\underline{H}_2$CH$_2$N-), 2.90 (t, $J = 4.9$ Hz, 4H, -OCH$_2$C$\underline{H}_2$N-), 6.86 (s, 2H, -C$\underline{H}$=C<), 6.89 (d, $J = 8.5$ Hz, 4H, H-3, and H-5 of C_6H_4CN on Biz), 6.98 (d, $J = 8.5$ Hz, 4H, H-2, and H-6 of C_6H_4CN on Biz), 7.70–7.79 (m, 8H, H-3, H-4, and H-5 of C_6H_5 at *meso* position), 7.75 (d, $J = 8.3$ Hz, 2H, H-3, and H-5 of C_6H_4CN on olefin), 7.85–7.87 (m, 8H, H-2, and H-6 of C_6H_5 at *meso* position), 8.24 (d, $J = 8.3$ Hz, 2H, H-2, and H-6 of C_6H_4CN on olefin), 8.97 (d, $J_{P-H} = 2.9$ Hz, 8H, pyrrole β); HRMS Calcd for

Table 1 Characterization of the Biz chromophore (**2**)

2	R	Ar	L	λ_{max}/nm[a]	λ_{EM}/nm (E^{0-0}/eV)[b]	$\Phi_2/10^{-2}$[c]	τ_2/ns[d]	$E_{1/2}^{ox}/V$[e]
2a	CF_3	Ph	CH_2	374	463 (2.68)	1.03	0.23	1.43
2b	CN	Ph	OCH_2CH_2	384	472 (2.63)	7.45	0.50	1.26
2c	CN	4-NCC_6H_4	OCH_2CH_2	382	451 (2.75)	7.63	0.78	1.35
2d	OH	Ph	CH_2	394	453 (2.74)	0.014	—	0.95

[a]Absorption maxima

[b]Emission maxima. The values in parentheses correspond to the excitation energy calculated from the emission spectra

[c]Fluorescence quantum yields from the Biz chromophore

[d]Fluorescence lifetime

[e]Oxidation potential vs. $Ag/AgNO_3$

$C_{88}H_{62}N_{12}O_6P^+$ [M^+]: 1413.4647, *m/z* 1413.4647. Found: 1413.4646.

Measurement of fluorescence quantum yields

The fluorescence (FL) spectra of solutions were measured using a Shimadzu RF-5300PC spectrometer. The FL spectra of **2a**–**2d** were measured at room temperature under excitation at 370 nm. The emission maxima (λ_{EM}) appeared near 460 nm. The concentrations of the solutions of **2** were adjusted so that the absorbance was <0.10 at the excitation wavelength. According to the reported method (Birks 1970), the quantum yield (Φ_2) of **2** was determined in MeOH using a solution of quinine bisulfate in 0.5 M H_2SO_4 with a quantum yield of 0.546 under excitation at 370 nm (Brouwer 2011). Table 1 shows the Φ_2 values.

In addition, the FL spectra of **1a**–**1c** were measured in MeOH under excitation of the P-porphyrin (Ptp) and Biz units at 550 and 370 nm, respectively. An MeCN solution of Zn (II) tetraphenylporphyrin (Zn(tpp)) with a fluorescence quantum yield of 0.029 (Sirish and Maiya 1994) was used as an actinometer for excitation at 550 nm. Table 2 lists the quantum yields (Φ_1^{Ptp} and Φ_2^{Ptp}) of FL data from Ptp at 610 nm under excitation of Ptp of **1** at 550 nm and 370 nm, respectively. The quantum yield of FL stemming from Biz at 460 nm under excitation of **1** at 370 nm is denoted as Φ_2^{Biz}.

Measurement of fluorescence lifetimes

Time-resolved fluorescence spectra were measured via the single photon counting method, using a streakscope (Hamamatsu Photonics, C4334-01) equipped with a polychromator (Acton Research, SpectraPro150) (Fujitsuka et al. 2004). An ultrashort laser pulse was generated using a Ti:sapphire laser (Spectra-Physics, Tsunami 3941-M1BB, full width at half maximum = 100 fs) pumped with a diode-pumped solid-state laser (Spectra-Physics, Millennia VIIIs). For excitation of the sample, the output of the Ti:sapphire laser was converted to second harmonic generation (430 or 370 nm) using a harmonic generator (Spectra-Physics, GWU-23FL) or a type I BBO (β-BaB_2O_4) crystal, respectively. The fluorescence lifetime of **2** (τ_2) was measured under excitation at 370 nm. The lifetimes (τ_1^{Ptp} and τ_2^{Ptp}) of the fluorescence from the Ptp moiety of **1** were measured under excitation of Ptp and Biz at 430 and 370 nm, respectively. Tables 1 and 2 summarize the obtained results.

Table 2 Quantum yield and lifetime of the fluorescence of **1a**–**1c**

	Excitation of Biz at 370 nm			Excitation of Ptp at 550 nm
	$\Phi^{Biz}/10^{-3}$[a]	$\Phi_2^{Ptp}/10^{-3}$ (τ_2^{Ptp}/ns)[b]	Φ_{ent}[c]	$\Phi_1^{Ptp}/10^{-2}$ (τ_1^{Ptp}/ns)[d]
1a	0.062	2.05 (5.08)	0.044	4.62 (5.13)
1b	0.47	1.87 (5.08)	0.046	4.07 (5.08)
1c	0.77	1.98 (5.08)	0.051	4.29 (4.50)

[a]FL quantum yield (Φ^{Biz}) from Biz (460 nm) under excitation of Biz at 370 nm. Lifetime of FL from Biz was not measured due to weak FL intensity

[b]FL appeared at 610 nm. Quantum yield (Φ_2^{Ptp}) and lifetime (τ_2^{Ptp}) of the FL from Ptp under excitation of Biz at 370 nm

[c]Energy transfer efficiency (Φ_{ent}) from Biz* to Ptp

[d]FL appeared at 610 nm. Quantum yield (Φ_1^{Ptp}) of FL from Ptp under excitation at 550 nm. The lifetime (τ_1^{Ptp}) was measured under excitation at 430 nm

Results and discussion

Design of P-porphyrins (1) with Biz on the axial positions

GFP is a biologically applicable fluorescent protein that contains the *p*-hydroxybenzylidene imidazolonyl chromophore depicted in Scheme 3, which is constructed via the condensation of glycine, tyrosine, and serine (Craggs 2009; Phillips Jr 1997). However, in the case of **2d** with R=OH, the fluorescence quantum yield (Φ_{2d}) was very weak (1.4×10^{-4}), as shown in Table 1. The P-porphyrin is a strong electron-accepting porphyrin due to the presence of

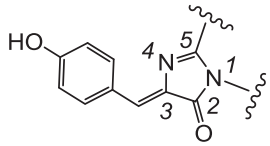

Scheme 3 Chromophore in GFP

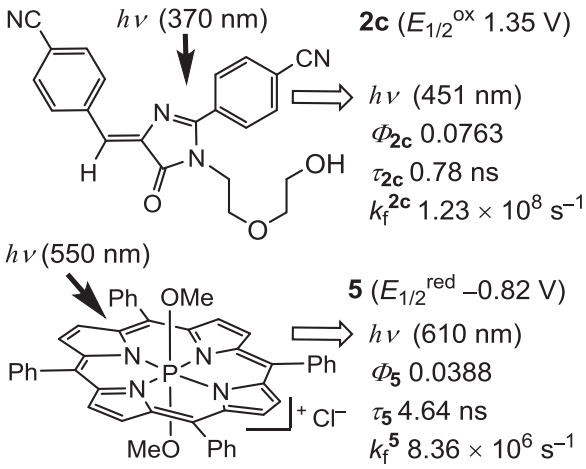

Scheme 4 Fluorescence parameters of **2c** and **5** in MeOH

pentavalent phosphorus. Indeed, the reduction potential of P-porphyrin was positively shifted compared with that of other metalloporphyrins; e.g., the $E_{1/2}^{red}$ values of dimethoxy(tetraphenylporphyrinato)phosphorus chloride (**5**, Scheme 4) and Zn(tpp) are −0.82 V (Shiragami et al. 2005) and −1.31 V (Felton and Linschitz 1966), respectively. This suggests that electron transfer between Biz and Ptp moieties may readily occur. Therefore, we introduced the electron-accepting CF_3 group in Biz (Follenius-Wund et al. 2003), obtaining **2a**. However, the Φ_{2a} of **2a** was still low (1.03×10^{-2}, Table 1). Therefore, R of Biz was changed from CF_3 to CN, thereby producing **2b**. In the case of **2c**, the CN group was introduced on both benzylidene and 5-phenyl moieties, and the Φ_2 values for both **2b** and **2c** were enhanced to $7.45–7.63 \times 10^{-2}$. Then next, the prepared **2a**–**2c** compounds were connected with Ptp through the linker (L) to produce **1a**–**1c**, respectively. In the cases of **1b** and **1c**, di(ethylenedioxy) group was used as L to weaken the intramolecular interaction between Biz and Ptp effectively.

Fluorescence of 1 under excitation of Biz

Figure 1 shows the FL spectra of **1a**–**1c** under selective excitation of the Biz moiety with 370 nm light. Two peaks attributable to the excited singlet state of Biz and Ptp (Biz* and Ptp*) at 460 and 610 nm, respectively, were observed. As can be seen in Table 2, the FL quantum yields (Φ^{Biz}) for the FL from the Biz* unit of **1a**–**1c** are about 1/100 of the Φ_2 values of **2a**–**2c**, suggesting the occurrence of the intramolecular quenching of Biz* by Ptp. The Φ^{Biz} values

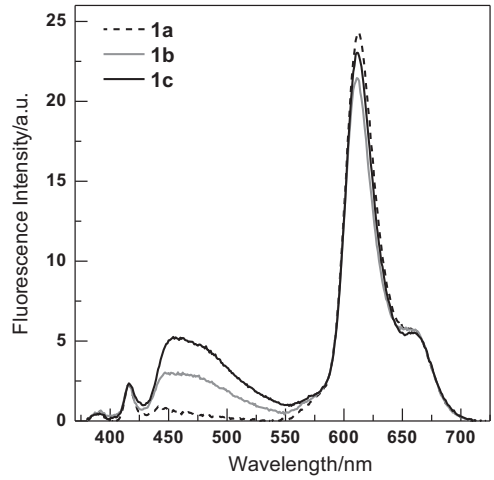

Fig. 1 Fluorescence spectra of **1a**–**1c** under excitation of Biz at 370 nm. The emissions at 450 and 610 nm can be attributed to the fluorescence from the Biz and Ptp chromophores, respectively

were dependent on R, with the largest value corresponding to **1c** (7.7×10^{-4}). Under excitation of Biz at 370 nm, the FL from Ptp* appeared at 610 nm in Φ_2^{Ptp}. Ptp* is most likely formed by energy transfer from Biz* to Ptp; the energy transfer efficiency (Φ_{ent}) was calculated to be 4.4–5.1% for **1a**–**1c** according to Eq. (1), using Φ_1^{Ptp} for FL from Ptp under excitation of the Ptp unit of **1**.

$$\Phi_{ent} = \frac{\Phi_2^{Ptp}}{\Phi_1^{Ptp}} \quad (1)$$

Analysis of the fluorescence spectra of 1c

Kinetic analysis was performed on **1c** due to its highest Φ^{Biz} among the P-porphyrins **1**. Compound **2c** was used as a reference of Biz without the Ptp chromophore. The fluorescence rate constants (k_f^{2c}) from the excited singlet states of **2c** were calculated to be $1.23 \times 10^8\ s^{-1}$ using Eq. (2). The rate constant (k_q) for the intramolecular quenching of Biz* by the Ptp unit in **1c** was calculated to be $1.26 \times 10^{11}\ s^{-1}$ (= $(0.0763/0.00077-1)/0.78 \times 10^9$) according to Eq. (3). The k_q value was extremely large compared with k_f^{2c}. In the quenching process, the participation of the energy transfer from Biz* to Ptp was small, considering the small Φ_{ent} value. Therefore, it seems reasonable to assume that the intramolecular quenching of Biz* by Ptp occurred mainly through electron transfer, which was an exothermic process with −0.58 eV according to the Rehm–Weller equation Eq. (4) (Rehm and Weller 1970), in which the oxidation potential of **2c** ($E_{1/2}^{ox} = 1.35$ V, Table 1), the reduction potential ($E_{1/2}^{red} = -0.82$ V) of $[(MeO)_2P(tpp)]Cl$ (**5**) (Shiragami et al. 2005), and the excitation energy of **2c** (E^{0-}

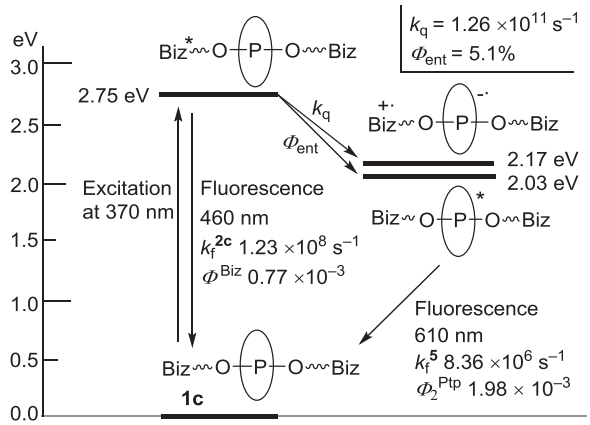

Scheme 5 Energy diagram for the decay processes of **1c** under excitation of Biz at 370 nm

$^0 = 2.75$ eV) calculated from the emission maximum of **2c** (451 nm, Table 1), were used.

$$k_f^{2c} = \frac{\Phi_{2c}}{\tau_{2c}} \qquad k_f 5 = \frac{\Phi 5}{\tau 5} \tag{2}$$

$$k_q = \frac{\left(\frac{\Phi_{2c}}{\Phi^{Biz}} - 1\right)}{\tau_{2c}} \tag{3}$$

$$\Delta G = E_{1/2}^{ox} - E_{1/2}^{red} - E^{0-0} \tag{4}$$

On the other hand, the Ptp* unit of **1c** was not quenched by Biz, as the Φ_1^{Ptp} and τ_1^{Ptp} values of **1c** were nearly identical as those of **5** (Φ_5 and τ_5), which was used as a reference compound of P-porphyrin without the Biz chromophore. The electron transfer from Ptp* to Biz was energetically unfavorable because the electron transfer from Biz to Ptp* was endothermic (+0.14 eV) (Scheme 5), which suggests that Ptp* decayed through a unimolecular process. The fluorescence rate constants of the Ptp* of **1c** were expected to be identical to those of **5*** (k_f^5), which were calculated to be 8.36×10^6 s^{-1} from Eq. (2) using Φ_5 and τ_5. On the basis of these parameters, a decay process for **1c** was constructed in Scheme 5.

The results described herein demonstrate that the introduction of Biz on the axial ligands of P-porphyrin did not affect the physicochemical properties of the Ptp chromophore, thereby evidencing the potential of compound **1c** to simultaneously act as sensitizer to generate singlet oxygen and as a fluorescent probe through its Ptp and Biz moieties, respectively.

Conclusion

A series of P-porphyrin complexes linked with the Biz chromophore through axial ligands were successfully synthesized. The excited state of the Biz unit of **1** was efficiently quenched by the Ptp moiety, resulting in weak fluorescence from Biz. The fluorescence quantum yield from Biz in **1** was enhanced up to 7.7×10^{-4} by introducing the CN group in Biz.

Acknowledgements This work was supported by a Grant-in-Aid for Scientific Research (C) (16K05847) from the Japan Society for the Promotion of Science (JSPS).

Compliance with ethical standards

Conflict of interest The authors declare that they have no competing interests.

References

Birks JB (1970) Photophysical of Aromatic Molecules. John Wiley, New York, NY, Birks JB (ed)

Brouwer AM (2011) Standards for photoluminescence quantum yield measurements in solution (IUPAC technical report). Pure Appl Chem 83(12):2213–2228. https://doi.org/10.1351/PAC-REP-10-09-31

Craggs TD (2009) Green fluorescent protein: structure, folding and chromophore maturation. Chem Soc Rev 38(10):2865–2875. https://doi.org/10.1039/b903641p

Dąbrowski JM, Pucelik B, Regiel-Futyra A, Brindell M, Mazuryk O, Kyzioł A, Stochel G, Macyk W, Arnaut LG (2016) Engineering of relevant photodynamic processes through structural modifications of metallotetrapyrrolic photosensitizers. Coord Chem Rev 325:67–101. https://doi.org/10.1016/j.ccr.2016.06.007

Ethirajan M, Chen Y, Joshi P, Pandey RK (2011) The role of porphyrin chemistry in tumor imaging and photodynamic therapy. Chem Soc Rev 40(1):340–362. https://doi.org/10.1039/b915149b

Felton RH, Linschitz H (1966) Polarographic reduction of porphyrins and electron spin resonance of porphyrin anions1. J Am Chem Soc 88(6):1113–1116. https://doi.org/10.1021/ja00958a004

Follenius-Wund A, Bourotte M, Schmitt M, Iyice F, Lami H, Bourguignon JJ, Haiech J, Pigault C (2003) Fluorescent derivatives of the GFP chromophore give a new insight into the GFP fluorescence process. Biophys J 85(3):1839–1850. https://doi.org/10.1016/S0006-3495(03)74612-8

Fujitsuka M, Okada A, Tojo S, Takei F, Onitsuka K, Takahashi S, Majima T (2004) Rapid exciton migration and fluorescent energy transfer in helical polyisocyanides with regularly arranged porphyrin pendants. J Phys Chem B 108(32):11935–11941. https://doi.org/10.1021/jp047753i

Gomer CJ, Ferrario A (1990) Tissue distribution and photosensitizing properties of mono-L-aspartyl chlorin e6 in a mouse tumor model. Cancer Res 50(13):3985–3990

Josefsen LB, Boyle RW (2012) Unique diagnostic and therapeutic roles of porphyrins and phthalocyanines in photodynamic therapy, imaging and theranostics. Theranostics 2(9):916–966. https://doi.org/10.7150/thno.4571

Matsumoto J, Kai Y, Yokoi H, Okazaki S, Yasuda M (2016) Assistance of human serum albumin to photo-sensitized inactivation of *Saccharomyces cerevisiae* with axially pyridinio-bonded P-porphyrins. J Photochem Photobiol, B 161:279–283. https://doi.org/10.1016/j.jphotobiol.2016.05.024

Matsumoto J, Shinbara T, Tanimura SI, Matsumoto T, Shiragami T, Yokoi H, Nosaka Y, Okazaki S, Hirakawa K, Yasuda M (2011) Water-soluble phosphorus porphyrins with high activity for visible light-assisted inactivation of Saccharomyces cerevisiae. J

Photochem Photobiol, A 218(1):178–184. https://doi.org/10.1016/j.jphotochem.2011.01.002

Matsumoto J, Suemoto Y, Kanemaru H, Takemori K, Shigehara M, Miyamoto A, Yokoi H, Yasuda M (2017a) Alkyl substituent effect on photosensitized inactivation of Escherichia coli by pyridinium-bonded P-porphyrins. J Photochem Photobiol B: Biol 168:124–131. https://doi.org/10.1016/j.jphotobiol.2017.02.001

Matsumoto J, Suzuki K, Uezono H, Watanabe K, Yasuda M (2017b) Additive effect of heparin on the photoinactivation of *Escherichia coli* using tricationic P-porphyrins. Bioorg Med Chem Lett 27 (23):5258–5261. https://doi.org/10.1016/j.bmcl.2017.10.032

Matsumoto J, Suzuki K, Yasuda M, Yamaguchi Y, Hishikawa Y, Imamura N, Nanashima A (2017c) Photodynamic therapy of human biliary cancer cell line using combination of phosphorus porphyrins and light emitting diode. Bioorg Med Chem 25 (24):6536–6541. https://doi.org/10.1016/j.bmc.2017.10.031

Mehraban N, Freeman HS (2015) Developments in PDT sensitizers for increased selectivity and singlet oxygen production. Materials 8 (7):4421–4456. https://doi.org/10.3390/ma8074421

Phillips Jr GN (1997) Structure and dynamics of green fluorescent protein. Curr Opin Struct Biol 7(6):821–827. https://doi.org/10.1016/S0959-440X(97)80153-4

Plaetzer K, Krammer B, Berlanda J, Berr F, Kiesslich T (2009) Photophysics and photochemistry of photodynamic therapy: fundamental aspects. Lasers Med Sci 24(2):259–268. https://doi.org/10.1007/s10103-008-0539-1

Rehm D, Weller A (1970) Kinetics of fluorescence quenching by electron and H-atom transfer. Isr J Chem 8(2):259–271. https://doi.org/10.1002/ijch.197000029

Shiragami T, Matsumoto J, Inoue H, Yasuda M (2005) Antimony porphyrin complexes as visible-light driven photocatalyst. J Photochem Photobiol, C 6(4):227–248. https://doi.org/10.1016/j.jphotochemrev.2005.12.001

Sirish M, Maiya BG (1994) Quenching of fluorescence in a series of covalently linked porphyrin-dinitrobenzene compounds. J Photochem Photobiol A Chem 77(2-3):189–200. https://doi.org/10.1016/1010-6030(94)80043-X

Walker CL, Lukyanov KA, Yampolsky IV, Mishin AS, Bommarius AS, Duraj-Thatte AM, Azizi B, Tolbert LM, Solntsev KM (2015) Fluorescence imaging using synthetic GFP chromophores. Curr Opin Chem Biol 27:64–74. https://doi.org/10.1016/j.cbpa.2015.06.002